



Adsorption Properties and Mechanism of Cd²⁺ in Water by Zr-containing Silica Residue Purification

Wanting Chen¹, Han Zhang¹, Yu Liang², Hao Ding^{1*} and Sijia Sun¹

¹ Beijing Key Laboratory of Materials Utilization of Nonmetallic Minerals and Solid Wastes, National Laboratory of Mineral Materials, School of Materials Science and Technology, China University of Geosciences, Beijing, China, ² School of Materials Science and Technology, Shenyang University of Chemical Technology, Shenyang, China

Zirconium (Zr)-containing silica residue purification (ZSR-P) discharged from industrial production of ZrOCl₂ was used as an adsorbent, and CdCl₂ solution was used as the simulated wastewater containing cadmium ions (Cd²⁺). The properties and mechanisms of ZSR-P absorbing Cd²⁺ were studied. The results showed that ZSR-P had a good effect on the adsorption and removal of Cd²⁺ in water. The adsorption time, initial concentration of Cd²⁺, and pH of the solution had a significant effect on the adsorption behavior, whilst the pH value had the greatest effect amongst them. Under optimal conditions, the amount of Cd²⁺ adsorbed by ZSR-P was 43.1 mg/g. The isothermal adsorption conformed to the Langmuir adsorption model, and the adsorption kinetics conformed to the secondary adsorption rate model. In ZSR-P-Cd, Cd²⁺ was uniformly distributed on the surface of SiO₂ particles and in the pores formed by the accumulation of particles. Adsorption of Cd²⁺ by ZSR-P was achieved through the reaction between Si-OH on the surface of SiO₂ and Cd²⁺ hydroxyl compounds.

Keywords: Zr-containing silica residue purification, adsorption, Cd²⁺, kinetic model, isothermal models

OPEN ACCESS

Edited by:

Wenbo Wang,
Lanzhou Institute of Chemical Physics
(CAS), China

Reviewed by:

Jianxi Zhu,
Guangzhou Institute of Geochemistry
(CAS), China
Shiyong Sun,
Southwest University of Science and
Technology, China

*Correspondence:

Hao Ding
dinghao113@126.com

Specialty section:

This article was submitted to
Green and Sustainable Chemistry,
a section of the journal
Frontiers in Chemistry

Received: 27 July 2018

Accepted: 29 October 2018

Published: 23 November 2018

Citation:

Chen W, Zhang H, Liang Y, Ding H
and Sun S (2018) Adsorption
Properties and Mechanism of Cd²⁺ in
Water by Zr-containing Silica Residue
Purification. *Front. Chem.* 6:556.
doi: 10.3389/fchem.2018.00556

INTRODUCTION

In recent decades, especially in some developing countries, the world economy has been growing rapidly. The process of industrialization, agricultural economy, and urbanization have been speeding up, which results in heavy metal pollution in water due to mining, metal smelting process, electroplating, and pesticide and fertilizer abuse. The excess emissions of sewage have become more critical than ever (Sekhar et al., 2004; Srivastava and Majumder, 2008; Fu and Wang, 2011; Huang et al., 2014). Heavy metal ions are the main water pollutants. They are easy, biologically enriched and hard to degrade and have high toxicity and stable chemical property, so their damage is extremely serious (Sha et al., 2010). Cadmium ion (Cd²⁺) is one of the most hazardous ions among these heavy metal ions. It has a strong chemical activity in the environment and can easily migrate into the food chain and endanger human health (Solenkova et al., 2014; Venza et al., 2014). Chronic exposure to Cd could cause great damage to cardiovascular system, nervous system, and livers of mammals and humans and may lead to renal failure and ultimately death (Romero-Gonzalez et al., 2001). For this reason, international regulatory agencies have issued wastewater standards for the discharge of various heavy metal ions, including Cd, to limit their entry into surface water and municipal sewers. However, due to the high cost of compliance with pollution control legislation, some small businesses cannot afford it. Therefore, some efficient, convenient, and cost effective processes need to be found for removing heavy metal ions from wastewater.

Currently, there are many available methods to remove heavy metals from the environment (Basci et al., 2004; Dabrowski et al., 2004; Ho and Ofomaja, 2006; Janin et al., 2009; Soyak et al., 2010), including oxidation reduction, chemical precipitation, ion exchange, membrane separation and adsorption, etc. Amongst these methods, oxidation reduction and chemical precipitation are traditional methods which cause some issues such as the large amount of chemical reagents, a secondary source of pollution to the environment, and poor treatment of low-concentration wastewater. Although the methods of ion exchange and membrane separation are effective, the processing scale is small and both the investment cost and operation cost are high. In contrast, the adsorption method, which is highly efficient and simple, suitable for renewable use and is applicable for low-concentration wastewater, requires low investment. Therefore, it is an attractive method with a vital potential for further development. At present, in addition to some nonmetallic minerals, the adsorbents used to treat the wastewater containing heavy metal ions also include activated carbon, humic acid adsorbents, macromolecule materials, biomaterials, and industrial solid wastes (Wong et al., 2003; Sprynskyy et al., 2006; Fan et al., 2007; Veli and Alyüz, 2007; Mohammad-Khah and Ansari, 2009). Bhattacharyya and Gupta (2008), Zhu et al. (2009), and Hong-Ping et al. (2001) studied the adsorption behavior of Cd²⁺ by using montmorillonite and kaolinite with the adsorption method and found that the adsorption capacity of different minerals for Cd²⁺ was different. However, since the surface area of the mineral material is not high, the amount of adsorption is reduced; therefore, a large amount of the adsorbent is required for the operation, which may cause a certain proportion of resources to be wasted. Bayat (2002) used fly ash as an adsorbent to adsorb Zn²⁺ and Cd²⁺ in wastewater. Because of its porous honeycomb structure and large surface area in the internal structure, it has a good adsorption capacity for various metal ions in wastewater. The unmodified fly ash needs to be chemically modified in order to improve its adsorption performance as the small number of functional groups contained on the surface invisibly increases the processing cost of the adsorption process, thus complicating it. The adsorption capacity of the modified fly ash can be compared with that of activated carbon, and the cost is only one third of the activated carbon.

Recently, more attention has been paid to low-cost adsorbents that can be used to replace carbonaceous and mineral materials. Industrial solid waste has become a hot adsorbent material because of its dual advantages in cost and technology. Zirconium (Zr)-containing silica residue is the solid gelatinous waste during industrial acid reaction process in the production of zirconium oxychloride (ZrOCl₂) from zirconite as the raw material. It is a loose-type gel. The main solid components of the gel are amorphous SiO₂ and a small amount of unreacted zirconite, crystalline NaCl, and other impurities. The main liquid components are water, some dissolved substances such as hydrochloric acid (HCl), ZrOCl₂, Na⁺, Cl⁻, and Fe³⁺, Zr⁴⁺, etc. In addition, the Zr-containing silica residue is purified to obtain Zr-containing silica residue purification (ZSR-P), which is mainly composed of amorphous SiO₂. It is expected to be an excellent adsorbent for the treatment of heavy metal ions in

the water by means of the surface charge properties of SiO₂, the characteristics of functional groups, and the pore channels formed by the accumulation of particles. This work undoubtedly has a positive significance for recycling solid waste and reducing the cost of wastewater treatment. However, very few reports have been made on the adsorption behavior and the thermodynamics of heavy metal ions by ZSR-P.

In this work, the adsorption behavior of Cd²⁺ from an aqueous solution using ZSR-P was studied by a set of experiments at various conditions, including temperature, adsorption time, initial concentration of Cd²⁺, and initial pH value. In order to identify the possible mechanisms involved in Cd²⁺ binding by ZSR-P, some characterization methods such as Fourier transform infrared spectrometer (FTIR) and X-ray photoelectron spectroscopy (XPS) were performed along with the analysis.

EXPERIMENTS

Raw Materials, Reagents, and Instruments

Zirconium-containing silica residue purification was obtained by purifying Zr-containing silica residue using a physical method. The Zr-containing silica residue raw material was produced by Henan Baililian Chemical Co. Ltd., Henan, China. The purification process involved the following steps. (1) The Zr-containing silica residue and water were added to a dispersing machine at a solid-liquid ratio of 7% to be crushed and mixed to form a uniform slurry. (2) The mixed slurry was pre-ground by an ultrafine grinder at 1,200 r/min. After 10 min, the alumina grinding balls were added to the mixed slurry at a ball ratio of 15:1. The grinding time was 35 min. (3) The mixed slurry containing the grinding balls was sieved to obtain the slurry. (4) The mixed slurry was separated by centrifugation, and each group of samples was centrifuged three times in order to obtain a gel of high purity containing amorphous silica. (5) The gel obtained after centrifugation was dried to finally obtain ZSR-P (Zhang et al., 2011). Additionally, ZSR-P had a specific surface area of 680.08 m²/g, and the pore diameter was 3.83 nm. The main chemical components before and after purification are shown in **Table 1**. The X-ray diffraction (XRD) analysis of ZSR-P is shown in **Figure 1**. It can be seen that a broad characteristic peak appears at a diffraction angle (2θ) of 20–25°, indicating that ZSR-P contains a large amount of amorphous phase components. In addition, there are no characteristic peaks of other impurities in the XRD pattern. So, combining with chemical analysis results (SiO₂ content of 94.63%), it suggests that the main component of ZSR-P should be amorphous SiO₂. Obviously, the properties of amorphous SiO₂ determine the performance of ZSR-P.

The CdCl₂ solution was used as the simulated wastewater containing Cd²⁺. A certain amount of solid CdCl₂ was weighed and added into distilled water, followed by stirring and dissolving to prepare the CdCl₂ solution with different Cd²⁺ contents. An NaOH solution of 0.1 mol/L or HCl of 0.1 mol/L was used for pH adjustment. All chemicals used were of analytical reagent grade and were obtained from Beijing Chemical Works, China.

The main test equipments used are described as follows. The adsorption reaction of ZSR-P on heavy metal simulated wastewater under different conditions was carried out by

using a SHZ-82 Thermostatic Bath Oscillator (Beijing Guohua Technology Group Ltd., Beijing, China). In addition, pH-3C (Inesa Analytical Instrument Co., Ltd, Shanghai, China) was used to adjust the pH of the reaction solution. Prodigy Inductively Coupled Plasma Atomic Emission Spectrometry (Leeman Labs INC., USA) was used to test the residual heavy metal ion content after the adsorption reaction. The potential of the surface before and after the adsorption of heavy metals by the adsorbent was tested by using a Zetasizer Nano ZS Potentiometer (Malvern Panalytical, UK). The structural characteristics of mesoporous materials were characterized by a specific surface area and porosity analyzer (BET, Quadrasorb Si-MP, Quantachrome, USA). The characterization was mainly at liquid nitrogen temperature (77K), and the relative pressure was $P/P_0 = 0 \sim 0.35$. The particle size, surface morphology, and elemental content distribution of ZSR-P were determined by using a scanning

electronic microscope combined with an energy dispersive X-ray detector (SEM-EDX, Hitachi High-Technologies Corporation, Tokyo, Japan). The particle size of the sample material and the comparative sample was observed using a FEI Tecnai G²F30 Field transmission electron microscope (TEM; acceleration voltage of 300 kV). The XRD analyses were conducted on a Rigaku D/max-rA (12 KW) X-ray powder diffractometer (XRD, D/MAX-2000, Rigaku Corporation, Tokyo, Japan) to determine the mineral composition operated with Cu K α radiation at 40 kV and 100 mA and with a scanning speed of 0.5° (2 θ)/min. A Fourier transform infrared spectroscope (FTIR, Perkin Elmer, Shanghai, China) was used to evaluate the distribution of functional groups on the surface between different materials. The XPS (Kratos Axis Ultra, UK) was used to characterize the surface composition and the combination state of the elements of ZSR-P before and after adsorption. Binding energies were referenced to the C1s peak at 284.8 eV. The oxide content and the elemental composition of the samples were analyzed by X-ray fluorescence (XRF) spectroscopy (S4-Explorer, Brukeraxs, Germany).

TABLE 1 | Comparison XRF of ZSR-P before and after purification.

ZSR		ZSR-P	
Analyte	Result (%)	Analyte	Result (%)
SiO ₂	81.8407	SiO ₂	92.7501
ZrO ₂	10.0438	ZrO ₂	4.7031
Cl	4.5786	Cl	1.2328
Na ₂ O	1.2677	Al ₂ O ₃	0.6939
CaO	0.4332	HfO ₂	0.2300
HfO ₂	0.3437	Na ₂ O	0.0951
Fe ₂ O ₃	0.3437	TiO ₂	0.0879
TiO ₂	0.3208	Fe ₂ O ₃	0.0733
Al ₂ O ₃	0.2688	Cr ₂ O ₃	0.0545
SO ₃	0.2032	K ₂ O	0.0411
MgO	0.1429	ThO ₂	0.0288
Y ₂ O ₃	0.0809	NbO	0.0094
Cr ₂ O ₃	0.0650		
ThO ₂	0.0396		
K ₂ O	0.0272		

Adsorption Experiments

The 100 ml Cd²⁺ solution with a known concentration was weighed and transferred into a 250 mL Erlenmeyer flask, regulating the pH value and adding a certain amount of ZSR-P into the suspension. The suspension was shaken for a certain period of time and then centrifuged to obtain a precipitate and a supernatant liquid, which were the ZSR-P products adsorbing Cd²⁺ (ZSR-P-Cd) and the Cd²⁺ removed from the solution, respectively. The Cd²⁺ content in the supernatant can be measured to evaluate the adsorption effect.

Characterization and Evaluation Method

(1) Calculation of adsorption amount

Inductively coupled plasma atomic emission spectrometry (ICP-AES) was used to determine the Cd²⁺ concentration of the supernatant after adsorption. The adsorption amount of Cd²⁺ by ZSR-P was calculated by the following formula:

$$q = \frac{(C_0 - C)V}{m}, \quad (1)$$

where C_0 and C are the initial concentration and residual concentration of Cd²⁺ in the solution, respectively, which are also called the concentrations before and after adsorption by ZSR-P (mg/L); q is the adsorption capacity of Cd²⁺ adsorbed by ZSR-P (mg/g); V is the solution volume (L); and m is the quality of ZSR-P added (g).

(2) Surface hydroxyl test

An amount of 2 g of the sample to be tested was weighed and placed in a 200 mL beaker, adding 75 mL of NaCl solution, which had a quality score of 0.2; 25 mL of absolute ethanol was added to the mixture, and then the mixture was stirred evenly with a magnetic stirrer. After adjusting the pH of the solution to 4 by using 0.1 mol/L NaOH or 0.1 mol/L HCl, 0.1 mol/L NaOH was added to raise the pH of the solution to 9 slowly and the pH value was kept unchanged for 20 s. The volume of NaOH used was recorded, and the

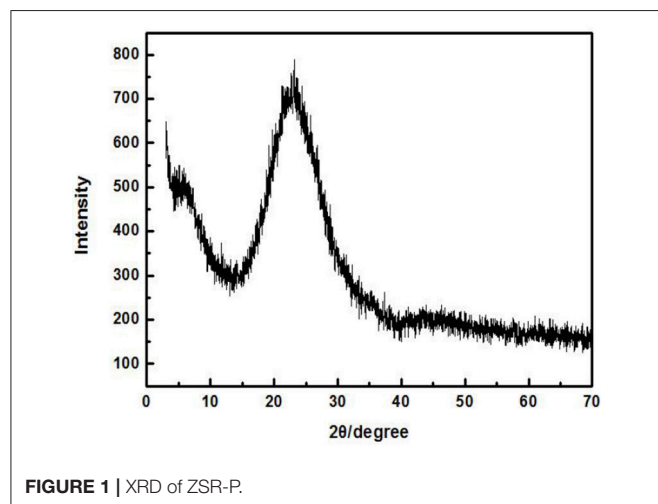


FIGURE 1 | XRD of ZSR-P.

number of hydroxyl groups N per square nanometer of the sample was calculated according to the following formula:

$$N = \frac{CVN_A \times 10^{-3}}{Sm}, \quad (2)$$

where C is the concentration of the NaOH solution (mol/L); V is the volume (L) of the NaOH solution; N_A is Avogadro's constant; S is the specific surface area of the sample (m²/g); and m is the mass of the sample (g).

RESULTS AND DISCUSSION

Study on Adsorption Properties

Effect of Temperature

The Cd²⁺ solution with a concentration of 100 mg/L (actual measured value was 94.97 mg/L by ICP-AES) was adjusted to an initial pH of 8. Later, 3 g/L of ZSR-P was added and heated to a certain temperature; the thermal insulation oscillation time was 10 min. **Figure 2** shows the effect of solution temperature on the adsorption of Cd²⁺ by ZSR-P. It can be seen that as the temperature rose from 25°C (room temperature) to 45°C, the amount of Cd²⁺ adsorbed by ZSR-P remained unchanged. When the temperature rose to 65°C, the adsorption amount increased slightly, indicating that temperature had little effect on the adsorption of Cd²⁺ by ZSR-P. According to the test results, considering the cost and operation conveniences for the treatment of the actual wastewater, the adsorption of the Cd²⁺ solution should be carried out at a temperature of 25°C, which is the normal temperature.

Adsorption Kinetics

The effect of the adsorption time on the adsorption of Cd²⁺ by ZSR-P is shown in **Figure 3**. The concentration of the Cd²⁺ solution used was 100 mg/L (actual measured value was 106.87 mg/L by ICP-AES), initial pH was 8, temperature was 25°C, and

ZSR-P dosage was 3 g/L. It can be seen from **Figure 3** that ZSR-P showed a fast adsorption behavior when the adsorption time was between 0 and 3 min. The adsorption time exceeded 3 min, and the adsorption capacity increased slowly and reached an equilibrium value at 7 min; the value was 22 mg/g. It showed that ZSR-P had a good effect on Cd²⁺ adsorption, and the effect of Cd²⁺ removal from the water was obvious.

According to the adsorption data of Cd²⁺ by ZSR-P in **Figure 3**, fitting was performed according to Lagergren quasi-first-order kinetic model and quasi-second-order kinetic model. The equations of the two models are as follows:

$$\text{Quasi - first - order kinetic model: } \log(Q_e - Q_t) = \log Q_e - \frac{K_1}{2.303} \bullet t \quad (3)$$

$$\text{Quasi - second - order kinetic model: } \frac{t}{Q_t} = \frac{1}{2K_2 \bullet Q_e^2} + \frac{t}{Q_e} \quad (4)$$

In the formula, Q_e is the quality (mg/g) of Cd²⁺ adsorbed by ZSR-P in solution during adsorption equilibrium; Q_t is the quality (mg/g) of Cd²⁺ adsorbed by ZSR-P in solution at adsorption time t ; and K_1 and K_2 are empirical factors.

Table 2 shows the parameters of the fitted kinetic equations. **Figure 4** compares the fitting curves and the distribution of the experimental data points. According to the quasi-first-order kinetic model, the correlation coefficient R^2 was only 0.035, indicating a low level of fitting degree. According to the quasi-second-order kinetic model, R^2 was as high as 0.999, indicating a high fitting degree. Obviously, the adsorption of Cd²⁺ by ZSR-P conformed to the pseudo-second-order kinetic model, and it also indicated that this adsorption was the surface adsorption reaction control process (Ho et al., 2000).

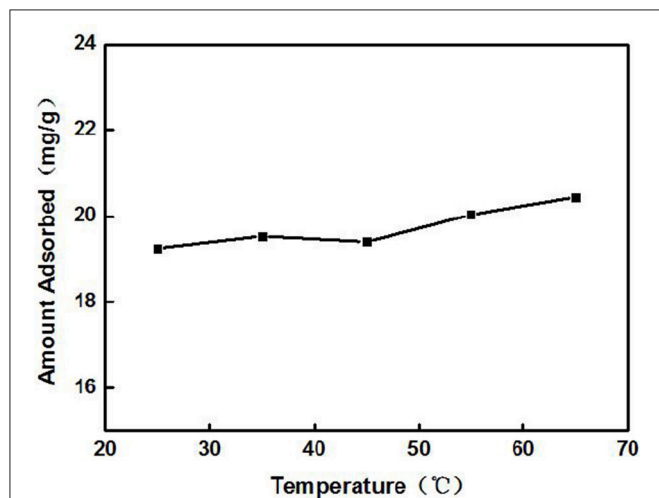


FIGURE 2 | Effect of solution temperature on adsorption of Cd²⁺ by ZSR-P.

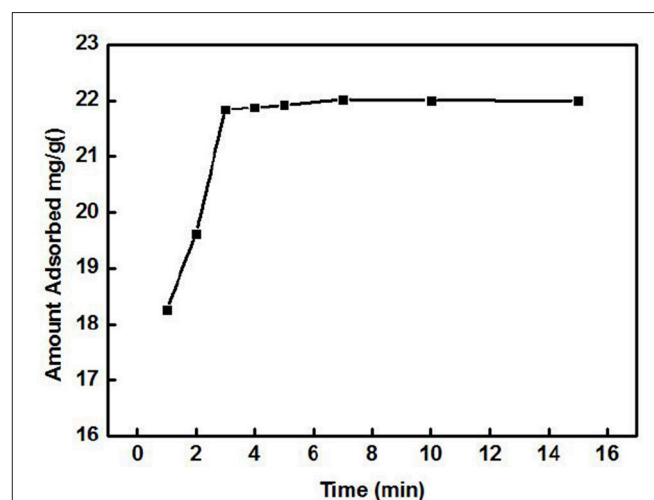


FIGURE 3 | Effect of solution time on adsorption of Cd²⁺ by ZSR-P.

Equilibrium Isotherms

Figure 5 shows the relationship between Cd²⁺ residual concentration (equilibrium concentration) in the solution and Cd²⁺ adsorption amount under the conditions of solution temperature 25°C, pH 8, ZSR-P dosage 3g/L, and adsorption time 15 min (In order to ensure that the adsorption reaction of Cd²⁺ by ZSR-P was fully balanced, the adsorption time was increased to 15 min), which is called the adsorption isotherm. It can be seen that with the increase in the concentration of Cd²⁺, the adsorption amount of Cd²⁺ by ZSR-P continued to increase until the concentration of Cd²⁺ was more than 80 mg/L; the stable value of the adsorption amount was 28 mg/g. According to the data in **Figure 5**, the isotherm of Cd²⁺ adsorbed by ZSR-P can be model-regressed. The Langmuir and Freundlich adsorption isothermal models commonly used are as follows.

Langmuir equation:

$$\frac{C_e}{Q_e} = \frac{1}{K_L Q_m} + \frac{C_e}{Q_m} \quad (5)$$

Freundlich equation:

$$\ln Q_e = \ln K_f + \frac{1}{n} \ln C_e \quad (6)$$

In the formula, C_e is the equilibrium concentration (mg/L) of Cd²⁺ adsorbed by ZSR-P in solution, Q_e is the adsorption amount (mg/g), Q_m is the saturated adsorption amount (mg/g), and K_L, K_f, and n are all empirical coefficients.

The data in **Figure 5** were processed and model-fitted to obtain the adsorption isotherm equations described by the

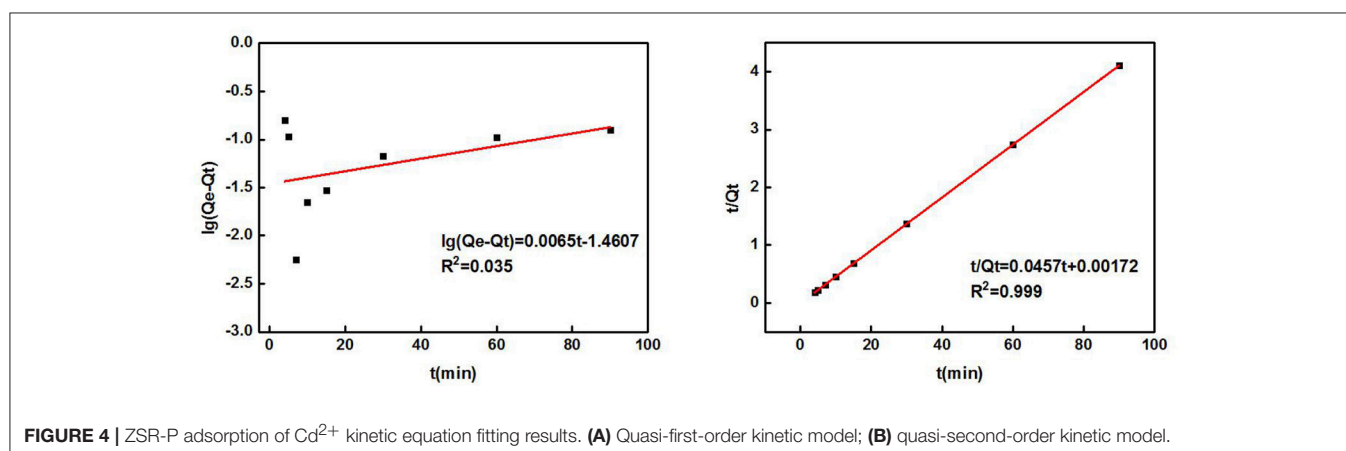
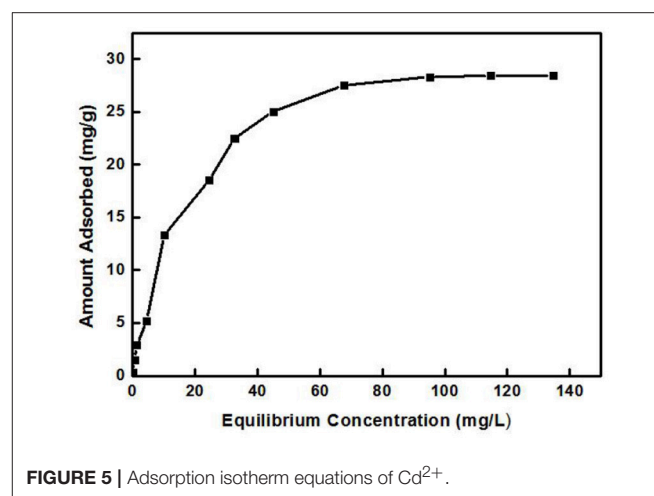
TABLE 2 | ZSR-P adsorption kinetic parameters of Cd²⁺.

Quasi-first-order kinetic model			Quasi-second-order kinetic model		
Q _e (mg/g)	K ₁	R ²	Q _e (mg/g)	K ₂	R ²
28.89	0.015	0.035	21.88	0.607	0.999

Langmuir and Freundlich models, as shown in **Table 3** and **Figure 6**. It can be seen that the correlation constants R² of the fitted Langmuir and Freundlich adsorption models were 0.994 and 0.85, respectively, indicating that the Langmuir model can better describe the adsorption isothermal behavior on Cd²⁺ by ZSR-P. The above results indicated that the adsorption of Cd²⁺ by ZSR-P was a monolayer adsorption, which indicated that the adsorption site was a single layer arrangement. The adsorption constant K_L was 0.058 (the value was small), indicating that the adsorption sites have a strong affinity (Langmuir, 2015).

Effect of pH

A 3 g/L solution of ZSR-P was added to the Cd²⁺ solution with different pH values under the conditions of solution Cd²⁺ concentration of 100 mg/L (actual measured value was 108.39 mg/L by ICP-AES) and temperature of 25°C, and then it was oscillated for 10 min to perform adsorption. **Figure 7** shows the effect of solution pH on adsorption. From **Figure 7**, it can be seen that the solution pH had a great influence on the adsorption of Cd²⁺ by ZSR-P. When pH value was less than 6, the adsorption



amount of Cd²⁺ was less than 10 mg/g, indicating that when pH was low, the adsorption of Cd²⁺ by ZSR-P was poor. When the pH was higher than 7, the adsorption amount increased greatly, and the maximum value was reached at pH 9, which was 43.1 mg/g. It showed that increasing the pH of the Cd²⁺ solution can greatly enhance the adsorption of Cd²⁺ by ZSR-P. The main reason was that Cd²⁺ was prone to hydrolysis at a higher pH, while ZSR-P has a stronger affinity to Cd²⁺ hydrolysate than free Cd²⁺ (Bayat, 2002). Obviously, the pH value of the solution was crucial for the adsorption of Cd²⁺ by ZSR-P.

TABLE 3 | Results of the fitting models of Cd²⁺ adsorption by ZSR-P.

Q _m	Langmuir model		Freundlich model		
	K _L	R ²	n	K _f	R ²
33.33	0.058	0.994	2.22	3.78	0.85

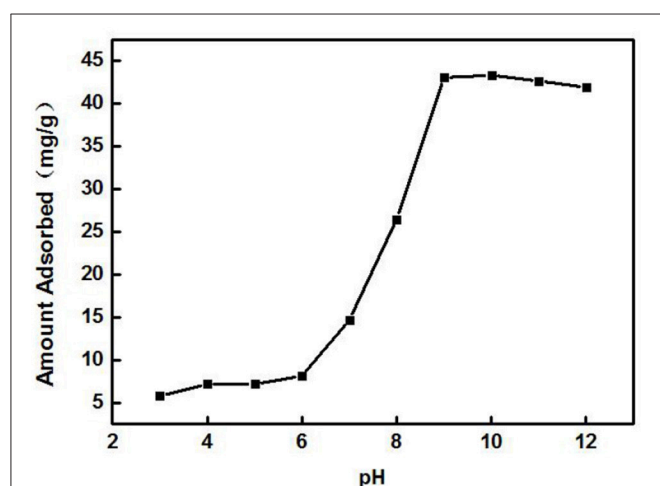


FIGURE 7 | Effect of pH on the adsorption of Cd²⁺ by ZSR-P.

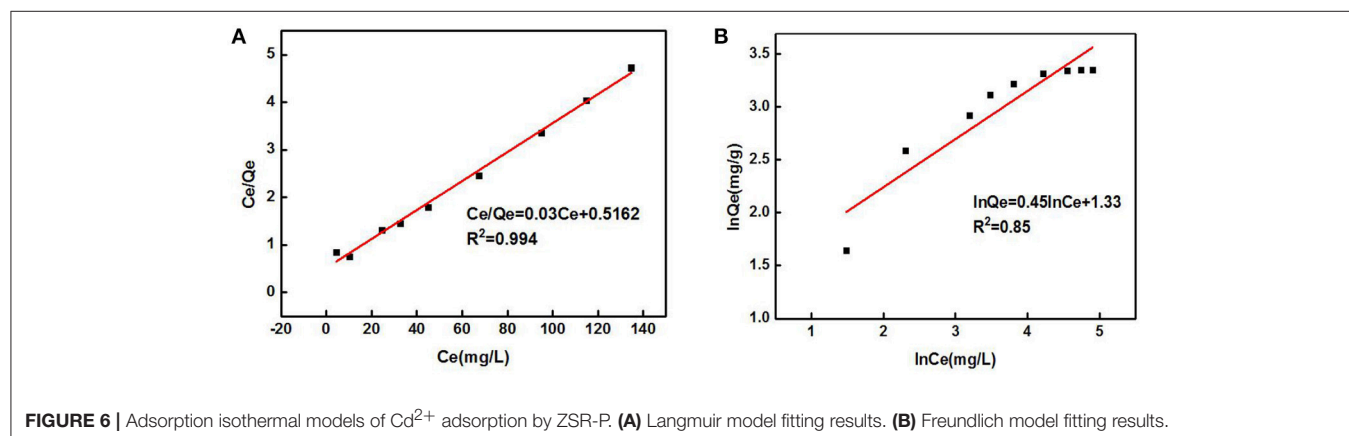


FIGURE 6 | Adsorption isothermal models of Cd²⁺ adsorption by ZSR-P. (A) Langmuir model fitting results. (B) Freundlich model fitting results.

ADSORPTION MECHANISM

Analysis of Adsorption Position

Figure 8 shows the SEM images and the surface distribution of the elements, such as O, Si, Zr, and Cd, of ZSR-P raw material and adsorbed Cd²⁺ product (ZSR-P-Cd). **Table 4** shows the energy spectrum analysis (EDX) values of each element on the surface. It can be seen that there was no Cd in the ZSR-P raw material while there was a large amount of Cd in ZSR-P-Cd, which was consistent with the test results of the adsorption amount of Cd²⁺. The distribution area of Cd was consistent with the position of ZSR-P particles in the SEM images, indicating that Cd²⁺ was uniformly adsorbed on the surface of SiO₂ particles in ZSR-P.

Figure 9 shows the TEM images of ZSR-P and ZSR-P-Cd. It can be clearly seen from **Figure 9A** that ZSR-P is mainly composed of aggregates formed by combining primary particles with sizes of about 20 nm. The small particles adhere to each other, and large aggregates of particles were formed. Due to the small particle size of the primary particles, ZSR-P had a large specific surface area, which was consistent with the test results. The large amount of hydroxyl groups present on the surface may provide a large number of adsorption and reaction binding sites for Cd²⁺. **Figure 9B** shows the TEM images of ZSR-P-Cd. It can be seen that the aggregated shape of ZSR-P-Cd particles was consistent with that of ZSR-P, indicating that no new substances were produced in the adsorption reaction. It was inferred that Cd²⁺ was adsorbed on the surface of ZSR-P and binding occurs between their interfaces.

Adsorbent Properties

Changes of Zeta Potential

The zeta potential is the difference between the shear plane of the solid-liquid relative movement and the potential inside the solution. The magnitude and the positive and negative values are determined by the solid surface properties, the Stern layer of the solid-liquid interface, the properties of the medium, and the concentration and nature of the ions in the solvation layer, which can reflect the difference in surface properties of ZSR-P before and after the adsorption of Cd²⁺ (Moreno-Castilla

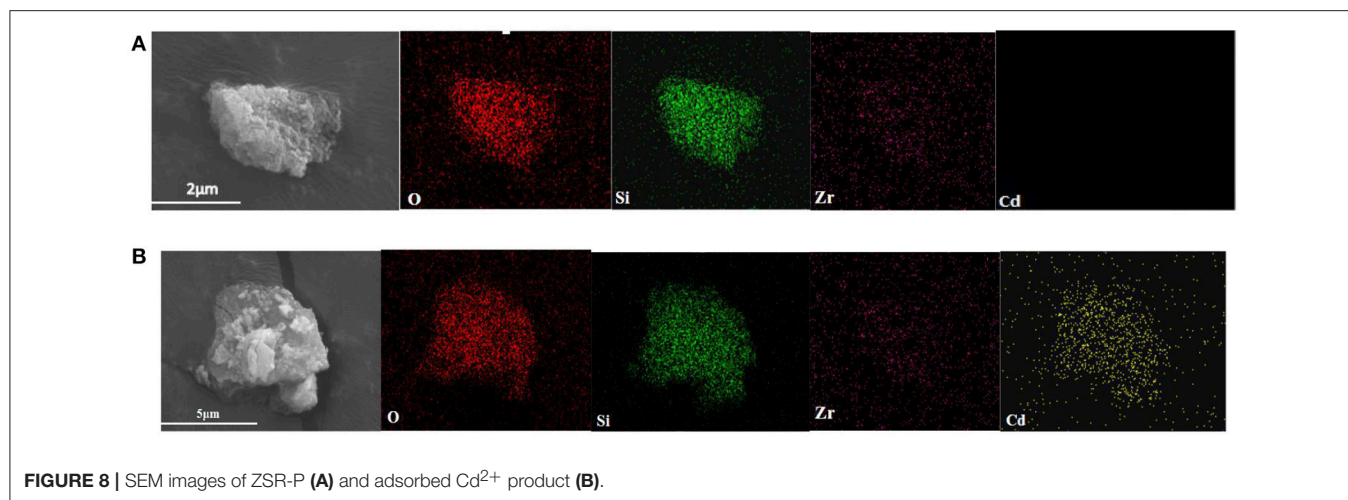
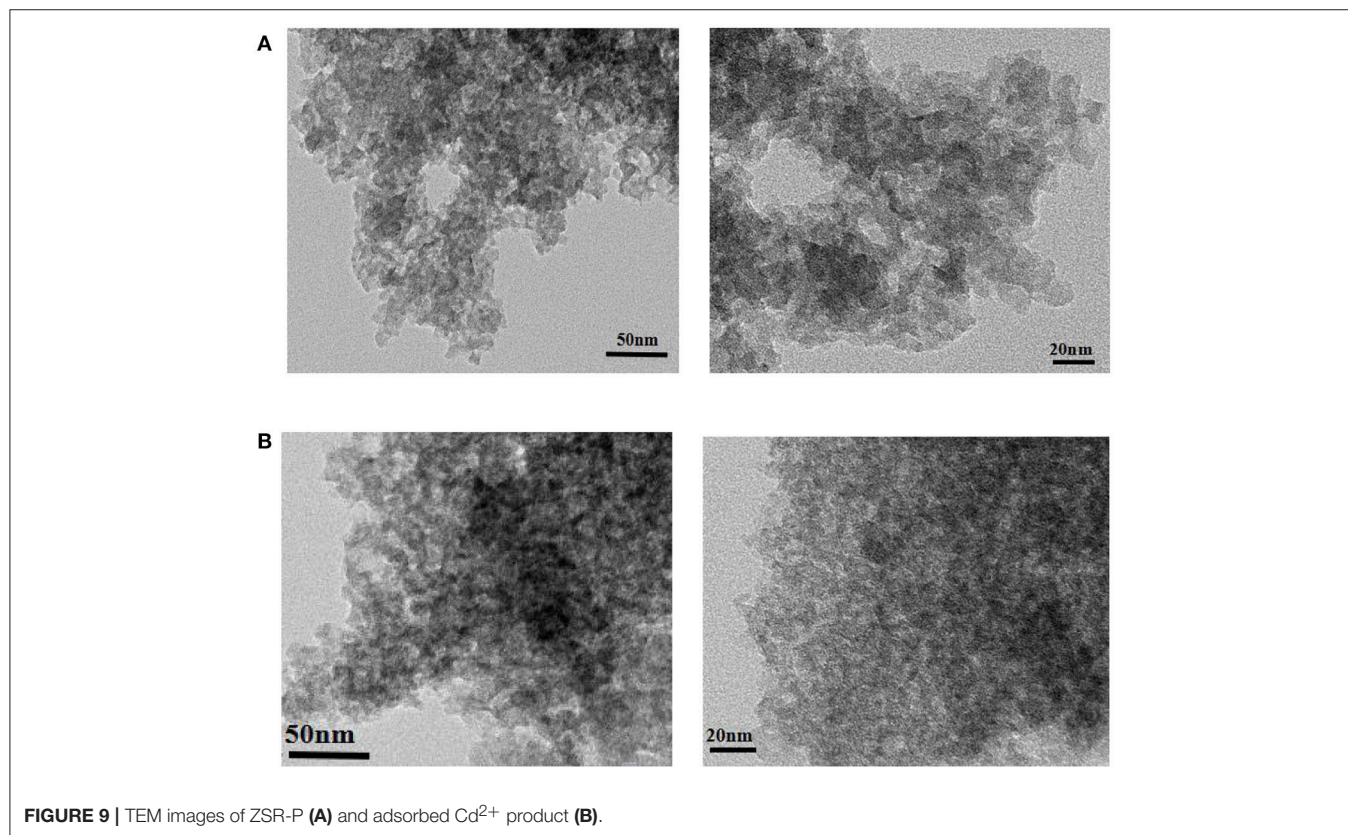


TABLE 4 | Elemental analysis of ZSR-P and adsorbed Cd²⁺ product.

Sample	O		Si		Zr		Cd	
	Atom fraction	Weight fraction						
ZSR-P	78.42	59.17	17.47	23.14	4.11	17.69	0	0
ZSR-P-Cd	76.90	54.64	18.10	22.58	2.32	9.41	2.68	13.37



et al., 2000, 2001). **Figure 10** shows the surface zeta potential values of ZSR-P raw materials and adsorbed Cd²⁺ products (ZSR-P-Cd) at different pH conditions. It can be seen that the zeta potential of the surface before and after the adsorption of Cd²⁺ by ZSR-P in the water system decreased with the increase in the pH value. When pH was less than 5.92, the zeta potential of the ZSR-P surface was positive, which indicated that the surface charge of ZSR-P was positive, and the counter ion of the Stern layer in the solution was negative. As the pH increased, the H⁺ ions in the solution gradually decreased, and the OH⁻ ions in the Stern layer and the diffusion layer of the ZSR-P surface gradually increased. The zeta potential of the ZSR-P surface was negative, and the absolute value gradually increased. When ZSR-P adsorbed Cd²⁺, the point of zero charge of ZSR-P-Cd shifted to the right to pH 6.7, indicating that more cations were adsorbed on the surface of the particles. When the pH was less than 6.7, the surface charge value of ZSR-P-Cd was larger than that of ZSR-P under the same pH condition. When the pH was greater than 6.7, the absolute surface charge value of ZSR-P-Cd was smaller than that of ZSR-P at the same pH.

Using the surface hydroxyl test method in formula (2), the surface hydroxyl groups before and after adsorption of Cd²⁺ by ZSR-P were 1.39/nm² and 1.06/nm², respectively. Therefore, it can be seen from the changes in surface zeta potential and hydroxyl density that under the same pH condition, the number of hydroxyl groups on the surface of the product after adsorption of Cd²⁺ were much smaller than that on the surface of ZSR-P. This indicates that when Cd²⁺ was added to the solution, ZSR-P was surrounded by a large number of cations in the solution, and the large amount of hydroxyl groups on the surface became the main binding site of the adsorption reaction; therefore, Cd²⁺ ions occupy the surface of the ZSR-P particles and the pores formed by the accumulation of particles.

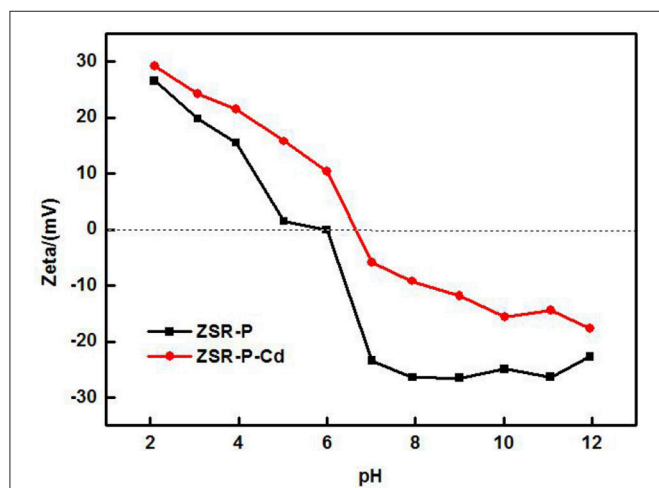


FIGURE 10 | Zeta potential of ZSR-P and adsorbed Cd²⁺ product.

Fourier Transform Infrared (FTIR) Spectroscopy

Figure 11 is the infrared spectra of ZSR-P and its adsorbed Cd²⁺ product (ZSR-P-Cd). In the infrared spectrum of ZSR-P, the peak at 3,438 cm⁻¹ was OH stretching of water; 1,637 cm⁻¹ was OH deformation of water; the strong absorption band caused by Si-O stretching appeared at 1,090 cm⁻¹ and 791 cm⁻¹; the peak at 970 cm⁻¹ belonged to Si-OH stretching; and the peak at 463 cm⁻¹ was Si-O-Si deformation, reflecting the characteristics of amorphous SiO₂ in ZSR-P. The peaks located at 1,637 cm and 3,438 cm were attributed by the abundant hydroxyl groups, which existing on the large specific surface area, absorb the surrounding water molecules. The comparison showed that the above absorption peaks appeared in the spectrum of ZSR-P adsorbed Cd²⁺ product except for the absorption peak at 970 cm⁻¹, and the peaks at 1,090 cm⁻¹ were slightly moved to 1,096 cm⁻¹. It was speculated that the Si-O stretching (Da-Qing et al., 2000) formed on the surface of SiO₂ hydrolyzed to form -SiOH (Bogdan et al., 1996) and combined with Cd²⁺ (d'espinoise de la Caillerie et al., 1997). The disappearance of the Si-OH stretching at 970 cm⁻¹ was presumed to be due to the dehydroxylation reaction on the surface of ZSR-P after the adsorption of Cd²⁺.

XPS Analysis

X-ray photoelectron spectroscopy analysis of ZSR-P and ZSR-P-Cd was performed, and the results are shown in **Figure 12**. The results show that the peaks of O, Si, and Zr appeared in the ZSR-P spectrum, reflecting the characteristics of ZSR-P being a component of SiO₂ and a small quantity of Zr-containing impurities. However, the peak of Cd3d_{5/2} appeared in the XPS of ZSR-P-Cd, and its binding energy was 405.72eV, indicating that Cd²⁺ was adsorbed on the surface of SiO₂, which was consistent with the results of SEM. In addition, the binding energies of Si2s and Si2p in the XPS of ZSR-P were 153.64 and 102.83 eV, respectively. While their binding energies in the XPS of ZSR-P-Cd were 154.07 and 103.04 eV, respectively. The larger binding energy value indicated that the chemical environment of Si had changed after the adsorption of Cd²⁺, which was consistent with

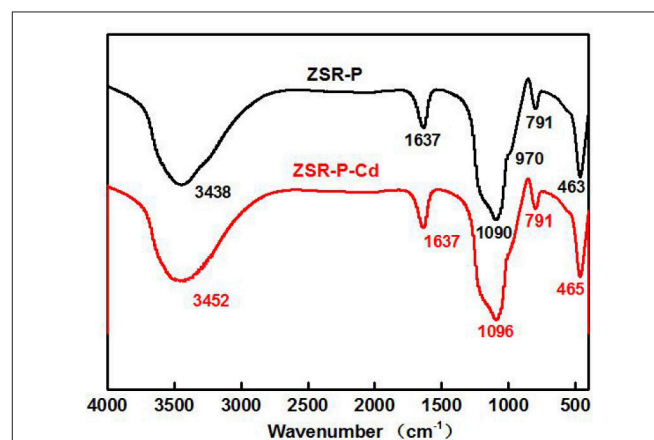


FIGURE 11 | Infrared spectra of ZSR-P and ZSR-P-Cd.

the results of Si-OH on the SiO₂ surface and Cd²⁺ hydrate reactions.

Adsorption Model

Based on the above analysis of the properties and mechanisms of ZSR-P adsorbing Cd²⁺, an interaction model reflecting this property, mechanism, and process was established and shown in Figure 13.

CONCLUSIONS

- (1) Zirconium-containing silica residue purification is mainly composed of aggregates of amorphous SiO₂ nanoparticles. It has an excellent adsorption and removal effect on Cd²⁺ in water. The pH value of the solution, Cd²⁺ concentration, and adsorption time have a significant effect on the removal effect. In addition, ZSR-P, at a dosage of 3 mg/L, was added to

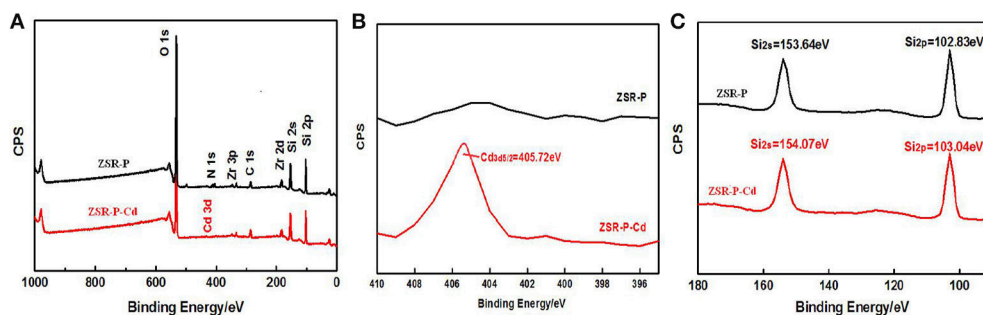


FIGURE 12 | XPS of ZSR-P and ZSR-P-Cd. **(A)** The XPS full spectrum of ZSR-P and ZSR-P-Cd. **(B)** The Cd3d spectrum of ZSR-P-Cd. **(C)** The Si2s and Si2p spectra of ZSR-P and ZSR-P-Cd.

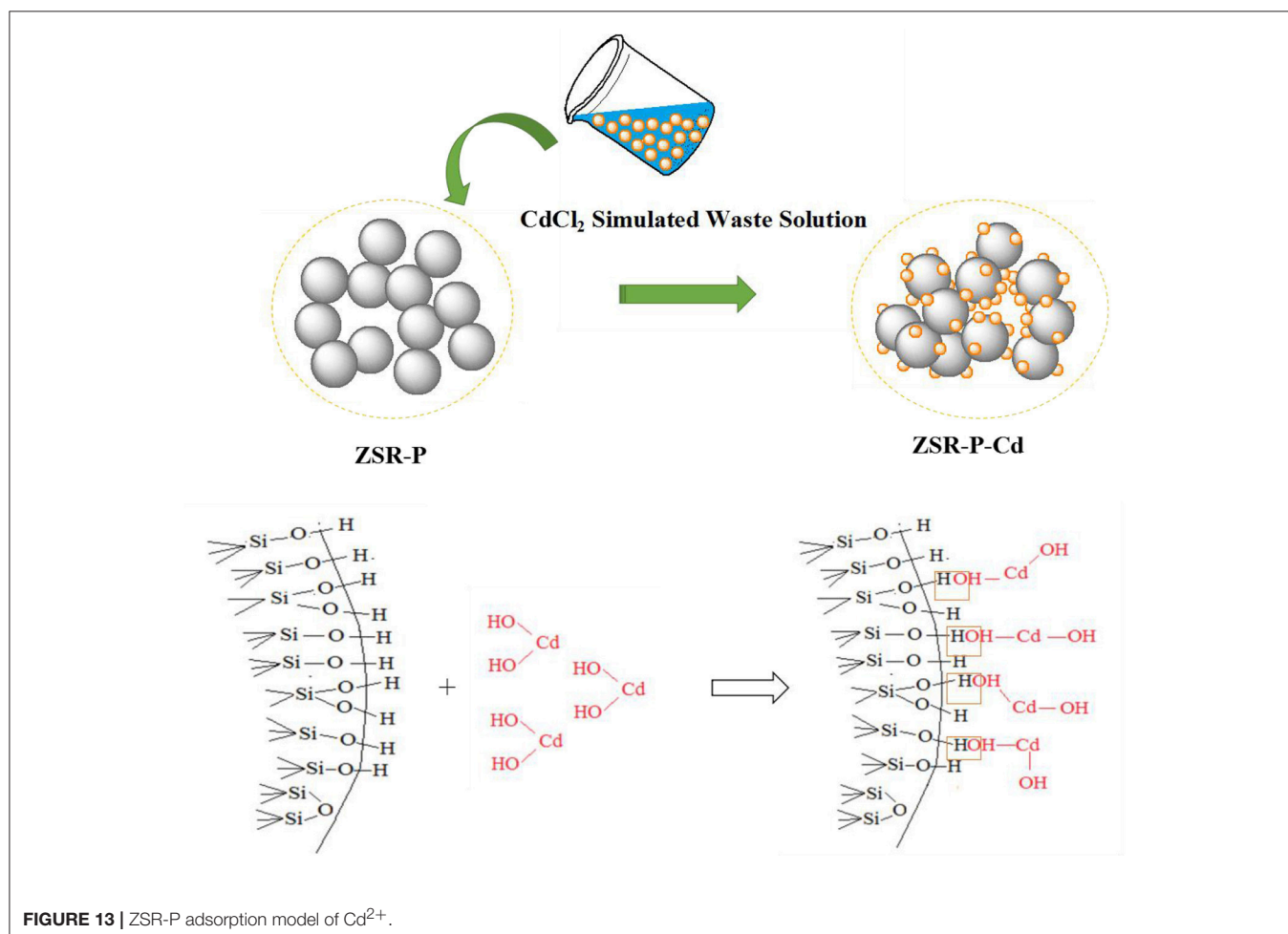


FIGURE 13 | ZSR-P adsorption model of Cd²⁺.

an aqueous solution, which had a Cd²⁺ concentration of 100 mg/L and pH 9, and then the mixture was shaken for 10 min; subsequently, the adsorption reached an equilibrium. The adsorption amount of Cd²⁺ by ZSR-P is 43.1 mg/g.

- (2) The isothermal adsorption of Cd²⁺ by ZSR-P is in accordance with the Langmuir adsorption model, consistent with the adsorption characteristics of general microporous materials. The adsorption kinetics equation of ZSR-P for Cd²⁺ conforms to the second-order model for adsorption rate.
- (3) The removal of Cd²⁺ in aqueous solution by ZSR-P is mainly based on the adsorption between them. In addition, Cd²⁺ is uniformly distributed on the surface of SiO₂ particles and in the pores formed by the accumulation of particles in ZSR-P-Cd. Adsorption between SiO₂ and Cd²⁺ is achieved by the

reaction between Si-OH on the surface of SiO₂ and Cd²⁺ hydroxyl compounds.

AUTHOR CONTRIBUTIONS

WC, HZ, HD, and SS conceived and designed the experiments. WC, HZ, and YL performed the experiments. WC and SS analyzed the data. HZ, YL, and SS contributed reagents. WC wrote the manuscript. YL retouched the document.

ACKNOWLEDGMENTS

The authors are thankful to the School of Materials Science and Technology, China University of Geoscience (Beijing), China for providing laboratory facilities.

REFERENCES

- Basci, N., Kocadagistan, E., and Kocadagistan, B. (2004). Biosorption of copper (ii) from aqueous solutions by wheat shell. *Desalination* 164, 135–140. doi: 10.1016/S0011-9164(04)00172-9
- Bayat, B. (2002). Combined removal of zinc (ii) and cadmium (ii) from aqueous solutions by adsorption onto high-calcium turkish fly ash. *Water. Air. Soil. Poll.* 136, 69–92. doi: 10.1023/A:1015296032528
- Bhattacharyya, K. G., and Gupta, S. S. (2008). Adsorption of a few heavy metals on natural and modified kaolinite and montmorillonite: a review. *Adv. Colloid. Interfac.* 140, 114–131. doi: 10.1016/j.cis.2007.12.008
- Bogdan, A., Kulmala, M., Gorbunov, B., and Kruppa, A. (1996). Nmr study of phase transitions in pure water and binary H₂O/HNO₃ films adsorbed on surface of pyrogenic silica. *J. Colloid. Interf. Sci.* 177, 79–87. doi: 10.1006/jcis.1996.0008
- Dabrowski, A., Hubicki, Z., Podkościelny, P., and Robens, E. (2004). Selective removal of the heavy metal ions from waters and industrial wastewaters by ion-exchange method. *Chemosphere* 56, 91–106. doi: 10.1016/j.chemosphere.2004.03.006
- Da-Qing, W. U., Diao, G. Y., Wei, J. F., and Yuan, P. (2000). Surface function groups and surface reactions of minerals. *Geol. J. China Univ.* 6, 225–226. doi: 10.16108/j.issn1006-7493.2000.02.019
- d'espinoise de la Caillerie J. B., Aimeur, M. R., Kortobi, Y. E., and Legrand, A. P. (1997). Water adsorption on pyrogenic silica followed by 1h mas nmr. *J. Colloid. Interf. Sci.* 194, 434–439. doi: 10.1006/jcis.1997.5126
- Fan, Z., Yu, B., Yue, Z., Wang, T., Xian, W., Liu, Z., et al. (2007). Preparation of porous chitosan gel beads for copper(ii) ion adsorption. *J. Hazard. Mater.* 147, 67–73. doi: 10.1016/j.jhazmat.2006.12.045
- Fu, F., and Wang, Q. (2011). Removal of heavy metal ions from wastewaters: a review. *J. Environ. Manage.* 92, 407–418. doi: 10.1016/j.jenvman.2010.11.011
- Ho, Y. S., Ng, J. C. Y., and McKay, G. (2000). Kinetics of pollutant sorption by biosorbents: review. *Separ. Purif. Method.* 29, 189–232. doi: 10.1081/SPM-100100009
- Ho, Y. S., and Ofomaja, A. E. (2006). Kinetic studies of copper ion adsorption on palm kernel fibre. *J. Hazard. Mater.* 137, 1796–1802. doi: 10.1016/j.jhazmat.2006.05.023
- Hong-Ping, H. E., Guo, J. G., Zhu, J. X., and Yang, D. (2001). An experimental study of adsorption capacity of montmorillonite, kaolinite and illite for heavy metals. *Acta Petrologica Et Mineralogica.* 20, 573–578.
- Huang, J., Lei, P., Zeng, G., Li, X., Zhao, Y., Liu, L., et al. (2014). Evaluation of micellar enhanced ultrafiltration for removing methylene blue and cadmium ion simultaneously with mixed surfactants. *Sep. Purif. Technol.* 125, 83–89. doi: 10.1016/j.seppur.2014.01.020
- Janin, A., Zaviska, F., Drogui, P., Blais, J. F., and Mercier, G. (2009). Selective recovery of metals in leachate from chromated copper arsenate treated wastes using electrochemical technology and chemical precipitation. *Hydrometallurgy* 96, 318–326. doi: 10.1016/j.hydromet.2008.12.002
- Langmuir, I. (2015). The adsorption of gases on plane surfaces of glass, mica and platinum. *J. Chem. Phys.* 40, 1361–1403. doi: 10.1021/ja02242a004
- Mohammad-Khah, A., and Ansari, R. (2009). Activated charcoal: preparation, characterization and applications: a review article. *Int. J. Chemtech. Res.* 1, 859–864.
- Moreno-Castilla, C., Carrasco-Mari, N. F., Parejo-Pérez, C., and Ramón, M. V. L. (2001). Dehydration of methanol to dimethyl ether catalyzed by oxidized activated carbons with varying surface acidic character. *Carbon.* 39, 869–875. doi: 10.1016/S0008-6223(00)00192-5
- Moreno-Castilla, C., López-Ramón, M. V., and Carrasco-Mari, N. F. (2000). Changes in surface chemistry of activated carbons by wet oxidation. *Carbon* 38, 1995–2001. doi: 10.1016/S0008-6223(00)00048-8
- Romero-Gonzalez, M. E., Williams, C. J., and Gardiner, P. H. (2001). Study of the mechanisms of cadmium biosorption by dealginated seaweed waste. *Environ. Sci. Technol.* 35, 3025–3030. doi: 10.1021/es991133r
- Sekhar, K. C., Chary, N. S., Kamala, C. T., Suman Raj D. S., and Sreenivasa Rao A. (2004). Fractionation studies and bioaccumulation of sediment-bound heavy metals in Kolleru lake by edible fish. *Environ. Int.* 29, 1001–1008. doi: 10.1016/S0160-4120(03)00094-1
- Sha, L., Guo, X. Y., Feng, N. C., and Tian, Q. H. (2010). Effective removal of heavy metals from aqueous solutions by orange peel xanthate. *T. Nonferr. Metal. So. C.* 20, 187–191. doi: 10.1016/S1003-6326(10)60037-4
- Solenkova, N. V., Newman, J. D., Berger, J. S., Thurston, G., Hochman, J. S., and Lamas, G. A. (2014). Metal pollutants and cardiovascular disease: mechanisms and consequences of exposure. *Am. Heart. J.* 168, 812–822. doi: 10.1016/j.ahj.2014.07.007
- Soylak, M., Unsal, Y. E., Kizil, N., and Aydin, A. (2010). Utilization of membrane filtration for preconcentration and determination of cu(ii) and pb(ii) in food, water and geological samples by atomic absorption spectrometry. *Food. Chem. Toxicol.* 48, 517–521. doi: 10.1016/j.fct.2009.11.005
- Sprynskyy, M., Buszewski, B., Terzyk, A. P., and Namieśnik, J. (2006). Study of the selection mechanism of heavy metal (Pb²⁺, Cu²⁺, Ni²⁺, and Cd²⁺) adsorption on clinoptilolite. *J. Colloid. Interf. Sci.* 304, 21–28. doi: 10.1016/j.jcis.2006.07.068
- Srivastava, N. K., and Majumder, C. B. (2008). Novel biofiltration methods for the treatment of heavy metals from industrial wastewater. *J. Hazard. Mater.* 151, 1–8. doi: 10.1016/j.jhazmat.2007.09.101

- Veli, S., and Alyüz, B. (2007). Adsorption of copper and zinc from aqueous solutions by using natural clay. *J. Hazard. Mater.* 149, 226–233. doi: 10.1016/j.jhazmat.2007.04.109
- Venza, M., Visalli, M., Biondo, C., Oteri, R., Agliano, F., Morabito, S., et al. (2014). Epigenetic effects of cadmium in cancer: focus on melanoma. *Curr. Genom.* 15, 420–435. doi: 10.2174/138920291506150106145932
- Wong, K. K., Lee, C. K., Low, K. S., and Haron, M. J. (2003). Removal of Cu and Pb by tartaric acid modified rice husk from aqueous solutions. *Chemosphere* 50, 23–28. doi: 10.1016/S0045-6535(02)00598-2
- Zhang, X. J., Ding, H., and Wang, B. K. (2011). Recycling and characterisation of amorphous silica from zr-containing silica residue. *Adv. Mater. Res.* 194–196, 2109–2114. doi: 10.4028/www.scientific.net/AMR.194-196.2109
- Zhu, X. P., Bai, D. K., Xi-Kun, L. I., Zeng, J. P., and Cao, S. Y. (2009). The adsorption behaviors of montmorillonite and some other clay minerals for cadmium. *Acta Petrologica Et Mineralogica.* 28, 643–648.

Conflict of Interest Statement: The authors declare that the research was conducted in the absence of any commercial or financial relationships that could be construed as a potential conflict of interest.

Copyright © 2018 Chen, Zhang, Liang, Ding and Sun. This is an open-access article distributed under the terms of the Creative Commons Attribution License (CC BY). The use, distribution or reproduction in other forums is permitted, provided the original author(s) and the copyright owner(s) are credited and that the original publication in this journal is cited, in accordance with accepted academic practice. No use, distribution or reproduction is permitted which does not comply with these terms.